

Al, B, and F doped $\text{LiNi}_{1/3}\text{Co}_{1/3}\text{Mn}_{1/3}\text{O}_2$ as cathode material of lithium-ion batteries

Shangyun Ye · Yongyao Xia · Pingwei Zhang ·
Zhiyu Qiao

Received: 27 March 2006 / Revised: 6 September 2006 / Accepted: 15 September 2006 / Published online: 21 November 2006
© Springer-Verlag 2006

Abstract A series of the mixed transition metal compounds, $\text{Li}[(\text{Ni}_{1/3}\text{Co}_{1/3}\text{Mn}_{1/3})_{1-x-y}\text{Al}_x\text{B}_y]\text{O}_{2-z}\text{F}_z$ ($x=0, 0.02, y=0, 0.02, z=0, 0.02$), were synthesized via coprecipitation followed by a high-temperature heat-treatment. XRD patterns revealed that this material has a typical $\alpha\text{-NaFeO}_2$ type layered structure with $R\bar{3}m$ space group. Rietveld refinement explained that cation mixing within the $\text{Li}(\text{Ni}_{1/3}\text{Co}_{1/3}\text{Mn}_{1/3})\text{O}_2$ could be absolutely diminished by Al-doping. Al, B and F doped compounds showed both improved physical and electrochemical properties, high tap-density, and delivered a reversible capacity of 190 mAh/g with excellent capacity retention even when the electrodes were cycled between 3.0 and 4.7 V.

Keywords Lithium-ion battery · Cathode materials · Doping · Layered structure

Introduction

Recently, the layer-structured $\text{Li}[\text{Ni}_{1/3}\text{Co}_{1/3}\text{Mn}_{1/3}]\text{O}_2$ positive electrode material was shown to be a possible

replacement for the commercial LiCoO_2 due to its low cost and high safety [1–4]. The rechargeable capacity of $\text{Li}[\text{Ni}_{1/3}\text{Co}_{1/3}\text{Mn}_{1/3}]\text{O}_2$ synthesized by a solid-state method is 150 mAh/g when the cell is operated at 2.5–4.3 V and close to 200 mAh/g on the voltage range of 2.5–4.6 V [1, 5]. An initial capacity of 160 mAh/g in the voltage window of 2.5–4.4 V was also reported for $\text{Li}[\text{Ni}_{1/3}\text{Co}_{1/3}\text{Mn}_{1/3}]\text{O}_2$ synthesized by mixed hydroxide method, but exhibits unstable cycling performance when charged to higher voltage (4.5 to 4.6 V) [6]. Moreover, a drawback of the low tap-density of the $\text{Li}[\text{Ni}_{1/3}\text{Co}_{1/3}\text{Mn}_{1/3}]\text{O}_2$ is that it may lead to low electrode density, thus resulting in low specific energy density of the practical Li-ion batteries.

It is well-known that the lithium-ion intercalation in the host of $\text{Li}[\text{Ni}_{1/3}\text{Co}_{1/3}\text{Mn}_{1/3}]\text{O}_2$ is associated with the redox reaction of Ni^{2+} to Ni^{4+} and Co^{3+} to Co^{4+} , while the Mn^{4+} do not participate in the redox reaction between 2.7 and 4.7 V [7, 8]. Choi et al. reported that lithium-rich compound, $\text{Li}_{1.03}(\text{Ni}_{1/3}\text{Co}_{1/3}\text{Mn}_{1/3})_{0.97}\text{O}_2$, showed better cycling stability and rate capability than that of the stoichiometric compound when it was charged to 4.6 V vs Li^+/Li [9]. Recently, we reported that partial replacement of the Mn site in $\text{Li}[\text{Ni}_{1/3}\text{Co}_{1/3}\text{Mn}_{1/3}]\text{O}_2$ with aluminum and lithium improved its electrochemical performance with a reversible capacity of 180 mAh/g, but showed poor cycling profile when charged to 4.6 V vs Li^+/Li [10]. Amatucci et al. observed that the formation of oxyfluoride, $\text{LiAl}_{0.2}\text{Mn}_{1.8}\text{O}_{3.8}\text{F}_{0.2}$, resulted in improvements in its capacity and retention during 300 cycles [11]. Kim et al. reported that both Mg and F doped $\text{Li}[\text{Ni}_{1/3}\text{Co}_{1/3}\text{Mn}_{1/3}]\text{O}_2$ showed enhancement in electrochemical performance [12]. Jouanneau et al. found that the high tap-density $\text{Li}[\text{Ni}_x\text{Co}_{1-2x}\text{Mn}_x]\text{O}_2$ powder could be obtained using an improved synthesis consisting of a well-controlled coprecipitation method [13, 14], or using B_2O_3 as a sintering agent [15].

S. Ye (✉) · Z. Qiao
Department of Physical Chemistry,
University of Science and Technology,
Beijing 100083, People's Republic of China
e-mail: yeys@superhoo.com

Y. Xia
Department of Chemistry, Fudan University,
Shanghai 200433, People's Republic of China

P. Zhang
Gejiu Superhoo Industries Limited Corporation,
Yunnan 661000, People's Republic of China

Therefore, the preparation of $\text{Li}[\text{Ni}_{1/3}\text{Co}_{1/3}\text{Mn}_{1/3}]_{\text{O}_2}$ with both improved electrochemical performance and high tap-density would appear to be of great interest. In the present work, we prepared a series of Al, B and F doped $\text{Li}[(\text{Ni}_{1/3}\text{Co}_{1/3}\text{Mn}_{1/3})_{1-x-y}\text{Al}_x\text{B}_y]\text{O}_{2-z}\text{F}_z$ ($x=0, 0.02, 0.02, z=0, 0.02$) by coprecipitation method, and the electrochemical performance was also evaluated as a positive electrode for Li-ion battery.

Materials and methods

Synthesis of the Al, B, and F doped $\text{LiNi}_{1/3}\text{Co}_{1/3}\text{Mn}_{1/3}\text{O}_2$ and related materials

NaOH (96%, Beijing Chemical Reagents), $\text{Ni}(\text{NO}_3)_2 \cdot \text{H}_2\text{O}$ (98%, Beijing Xinhua Reagent), $\text{Co}(\text{NO}_3)_3 \cdot \text{H}_2\text{O}$ (99%, Beijing Shuanghuan Reagents), and $\text{Mn}(\text{NO}_3)_2$ (50% aqueous solution, Beijing Xinhua Reagents) were used as starting materials. $\text{Ni}_{1/3}\text{Co}_{1/3}\text{Mn}_{1/3}(\text{OH})_2$ precursor was prepared by the coprecipitation method utilizing a chelating agent, as described in Ref. [10]. The $\text{Li}[(\text{Ni}_{1/3}\text{Co}_{1/3}\text{Mn}_{1/3})_{1-x-y}\text{Al}_x\text{B}_y]\text{O}_{2-z}\text{F}_z$ was prepared by solid synthesis method: $[\text{Ni}_{1/3}\text{Co}_{1/3}\text{Mn}_{1/3}]_3\text{O}_4$ was obtained by heat-treating the dried $\text{Ni}_{1/3}\text{Co}_{1/3}\text{Mn}_{1/3}(\text{OH})_2$ precursor at 500 °C for 5 h, and then mixed with a stoichiometric amount of $\text{LiOH} \cdot \text{H}_2\text{O}$ (95%, Beijing Xinhua Reagents), LiF (AR, Beijing Chemical Reagents), Al_2O_3 (AR, Beijing Chemical Plant), and B_2O_3 (AR, Beijing Chemical Reagents) using an automatic grinder. After grinding, pellets of 12 mm diameter and about 0.35 mm thickness were made, heated at 900 °C for 10 h, followed by annealing at 700 °C for 5 h in air. After quenching, the pellets were broken up and ground with the automatic grinder.

Characterisation of the samples

The crystalline phase of the samples was identified by powder X-ray diffraction (XRD) on a Rigaku D/MAX-RC X-ray diffractometer with $\text{Cu K}\alpha$ radiation. The obtained XRD data ($2\theta=10\text{--}130^\circ$) had a step size of 0.02° and a count time of 5 s and were analyzed by the Rietveld refinement using Fullprof 2000 [16]. A scanning electron microscopy (SEM) study of some representative samples was performed to obtain an understanding of their morphology. The images were made with a KYKY model 500 scanning electron microscope.

Electrode sheets were prepared by mixing 85 wt% active material, 10 wt% carbon black, and 5 wt% polyvinylidene fluoride binder (PVDF, dissolved in *N*-methyl-2-pyrrolidone, NMP) to form a slurry. The slurry was then cast on the aluminum foil with a typical thickness of about 66 μm . The cathode disks with a diameter of 12 mm were punched

out of the foil, and then dried in a vacuum oven at 120 °C to remove the solvent for 24 h.

Test cells were assembled and sealed in an Ar-filled glove box with doped or un-doped $\text{LiNi}_{1/3}\text{Co}_{1/3}\text{Mn}_{1/3}\text{O}_2$ as the working electrode, fresh lithium foil as the counter electrode, 1 M LiPF_6 dissolved in a mixture of ethylene carbonate (EC, battery grade) and dimethyl carbonate (DMC, battery grade) (1:1 by volume) was used as the electrolyte and Celgard 2400 polyethylene/polypropylene as the separator. Test cells for electrochemical performance evaluation of the positive electrode material were cycled between 3 V and various preset charge cutoff potentials (vs Li) galvanostatically on Land 2000T (Wuhan, China) with various current densities.

Results and discussion

Synthesis, micromorphology and tap-density

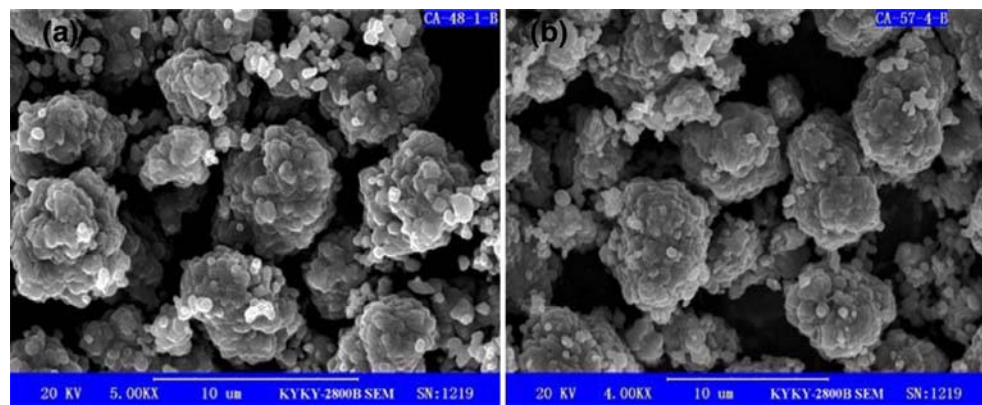
To prepare a homogeneous metal hydroxide, it is important to control the pH of the respective metal-containing aqueous solution. In the case of Mn, especially, the pH control is very critical since the precipitation of manganese oxide is favored by high temperature (>60 °C), hence, the pH of the solution was adjusted to the range at which manganese hydroxide would not precipitate. The contents of the elements in the $\text{Li}[(\text{Ni}_{1/3}\text{Co}_{1/3}\text{Mn}_{1/3})_{0.96}\text{Al}_{0.02}\text{B}_{0.02}]\text{O}_{1.98}\text{F}_{0.02}$ sample were obtained by inductively coupled plasma mass spectroscopy (ICPMS) and chemical analysis. The results given in Table 1 demonstrate that a well-stoichiometric amount of the sample was obtained.

Figure 1 shows the SEM images of the doped and undoped $\text{LiNi}_{1/3}\text{Co}_{1/3}\text{Mn}_{1/3}\text{O}_2$. Both the resulting compounds are comprised of spherical agglomerated particles. The particles size and shapes are more retained from the coprecipitated precursor during calcination and annealing, as previously discussed in Ref. [10]. The smaller sheet-shaped primary particles grow into square and spherical shapes through high-temperature calcination. The size and shape of the secondary particles scarcely change during the calcination process. The Al–B–F substituted samples have a well-defined square-shaped morphology and the non-porous body with a smooth crystal surface in primary particles (Fig. 1b). The average diameters of the secondary particles are about 8 μm . The Al–B–F doped compound

Table 1 Li, Ni, Mn, Co, Al, F in the $\text{Li}[(\text{Ni}_{1/3}\text{Co}_{1/3}\text{Mn}_{1/3})_{0.96}\text{Al}_{0.02}\text{B}_{0.02}]\text{O}_{1.98}\text{F}_{0.02}$ sample

Elements	Li	Ni	Mn	Co	Al	F
Content (mass%)	7.31	20.71	18.91	20.70	0.55	0.39

Fig. 1 SEM images of the prepared compounds. (a) $\text{Li}[\text{Ni}_{1/3}\text{Co}_{1/3}\text{Mn}_{1/3}]O_2$; (b) $\text{Li}[(\text{Ni}_{1/3}\text{Co}_{1/3}\text{Mn}_{1/3})_{0.96}\text{Al}_{0.02}\text{B}_{0.02}]O_{1.98}\text{F}_{0.02}$



delivers much tightly packed particles than that of the undoped compound. The measured tap-density are summarized in Table 2. Apparently, Al, B and F doped compounds show improved tap-density. The sintering effect of B_2O_3 is in good agreement with the result reported by Jouanneau et al. [15].

XRD measurements and Rietveld refinement

Figure 2 shows the powder XRD patterns of all compounds. All of the peaks can be indexed as a hexagonal lattice ($\alpha\text{-NaFeO}_2$ type, space group: $R\bar{3}m$, 166) even with total 4% atom Al and B doped. The resulting XRD peaks are narrow, indicating high crystalline. The XRD patterns of Al-doping and Al–B–F-doping samples (Fig. 2b and c) are quite similar to that of the un-doped sample (Fig. 2a). It is believed that all the Al, B and F atoms are being incorporated within the $\text{Li}[\text{Ni}_{1/3}\text{Co}_{1/3}\text{Mn}_{1/3}]O_2$ structure and that the solid solution of $\text{Li}[(\text{Ni}_{1/3}\text{Co}_{1/3}\text{Mn}_{1/3})_{1-x-y}\text{Al}_x\text{B}_y]\text{O}_{2-z}\text{F}_z$ is formed. The splits in the (006)/(012) and (018)/(110) doublets indicate the formation of a highly ordered layered structure, implying that the well-defined layered structure was achieved by Al–B–F substitution similar to the case of Al-doping only [10].

To shed some light on this issue, we employed the Rietveld method to analyze the crystal structure. A simultaneous refinement was carried out on the hexagonal

lattice ($\alpha\text{-NaFeO}_2$ type, space group: $R\bar{3}m$, 166) in which Li occupied the 3a sites, transition metal ions Al and B the 3b sites, and oxygen and fluorine atoms the 6c sites. We fixed the oxygen, fluorine occupations and assumed that the “cation mixing” (i.e. a partial interchange of occupancy of Li and transition metal ions among the sites) happened. Only Ni^{2+} was expected to exist in the lithium plane, as confirmed by neutron diffraction studies [17]. The refinement results are listed in Table 3.

Table 3 shows that the resulting lattice parameters and unit cell volume are decreased to about 1% by Al–B–F-doping like the case of Al-doping compared to $\text{Li}[\text{Ni}_{1/3}\text{Co}_{1/3}\text{Mn}_{1/3}]O_2$, but tap-density is increased to about 45% as seen in Table 2. The higher tap-density of the sample doped with Al–B–F may be attributed to the tightly packed primary particles because of the sintering effect of B_2O_3 [15].

As can be seen from the data of ion occupancy in Table 3, the “cation mixing” occurred within the $\text{Li}[\text{Ni}_{1/3}$

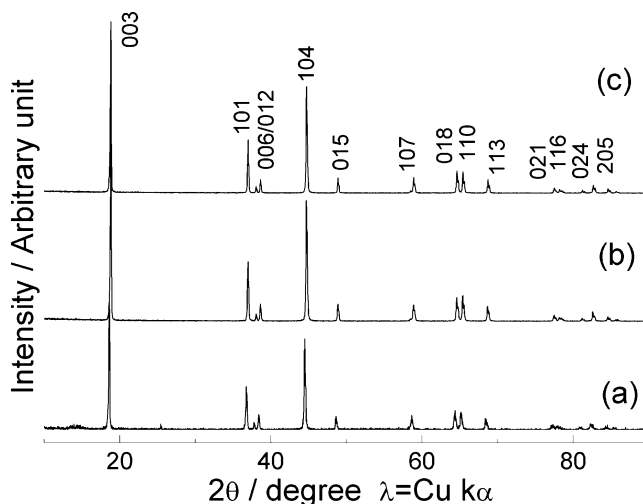


Fig. 2 Powder XRD patterns of the samples. (a) $\text{Li}[\text{Ni}_{1/3}\text{Co}_{1/3}\text{Mn}_{1/3}]O_2$; (b) $\text{Li}[(\text{Ni}_{1/3}\text{Co}_{1/3}\text{Mn}_{1/3})_{0.98}\text{Al}_{0.02}]O_2$; (c) $\text{Li}[(\text{Ni}_{1/3}\text{Co}_{1/3}\text{Mn}_{1/3})_{0.96}\text{Al}_{0.02}\text{B}_{0.02}]O_{1.98}\text{F}_{0.02}$

Table 2 Measured tap-densities and specific surface area

Samples	Tap-density (g/cm ³)	Specific surface area (m ² /g)
$\text{Li}[\text{Ni}_{1/3}\text{Co}_{1/3}\text{Mn}_{1/3}]O_2$	1.71	0.52
$\text{Li}[(\text{Ni}_{1/3}\text{Co}_{1/3}\text{Mn}_{1/3})_{0.98}\text{Al}_{0.02}]O_2$	2.12	0.43
$\text{Li}[(\text{Ni}_{1/3}\text{Co}_{1/3}\text{Mn}_{1/3})_{0.96}\text{Al}_{0.02}\text{B}_{0.02}]O_{1.98}\text{F}_{0.02}$	2.48	0.36

Table 3 Rietveld fitting parameters for the three kinds of compounds

Atom	Site	Li[(Ni _{1/3} Co _{1/3} Mn _{1/3}) _{0.96} Al _{0.02} B _{0.02}]O _{1.98} F _{0.02}	Li[(Ni _{1/3} Co _{1/3} Mn _{1/3}) _{0.98} Al _{0.02}]O ₂	Li(Ni _{1/3} Co _{1/3} Mn _{1/3})O ₂
		x y z Occupancy	x y z Occupancy	x y z Occupancy
Li	3a	0 0 0 0.99995	0 0 0 0.99988	0 0 0 0.9686
Ni	3a	0 0 0 0.00005	0 0 0 0.00012	0 0 0 0.0314
Li	3b	0 0 0.5 0	0 0 0.5 0	0 0 0.5 0.0314
Ni	3b	0 0 0.5 0.31995	0 0 0.5 0.32655	0 0 0.5 0.3019
Co	3b	0 0 0.5 0.32	0 0 0.5 0.32667	0 0 0.5 0.3333
Mn	3b	0 0 0.5 0.32	0 0 0.5 0.32667	0 0 0.5 0.3333
Al	3b	0 0 0.5 0.02	0 0 0.5 0.020	
B	3b	0 0 0.5 0.02		
O	6c	0 0 0.2408 1.98	0 0 0.2405 2	0 0 0.2428 2
F	6c	0 0 0.2408 0.02		
Lattice parameters		$a=2.8553 \text{ \AA}$, $c=14.2139 \text{ \AA}$ $V=100.358 \text{ \AA}^3$	$a=2.8560 \text{ \AA}$, $c=14.2234 \text{ \AA}$ $V=100.474 \text{ \AA}^3$	$a=2.8628 \text{ \AA}$, $c=14.2778 \text{ \AA}$ $V=101.358 \text{ \AA}^3$
		$R_{wp}=12.7\%$, $R_p=9.34\%$	$R_{wp}=11.4\%$, $R_p=8.44\%$	$R_{wp}=11.5\%$, $R_p=8.51\%$

a and *c* are the lattice constants of the structures. R_{wp} and R_p are the two quantities describing the goodness of fitting and the agreement between the calculated and observed intensities, respectively

Constraints: space group: $R\bar{3}m$ (no.166)

Total occupancy of 3a sites, $(\text{Li})_{3a}+(\text{Ni})_{3a}=1$

Total occupancy of 3b sites, $(\text{Ni})_{3b}+(\text{Mn})_{3b}+(\text{Co})_{3b}+(\text{Al})_{3b}+(\text{B})_{3b}=1$

Total occupancy of 6c sites, $(\text{O})_{6c}+(\text{F})_{6c}=2$

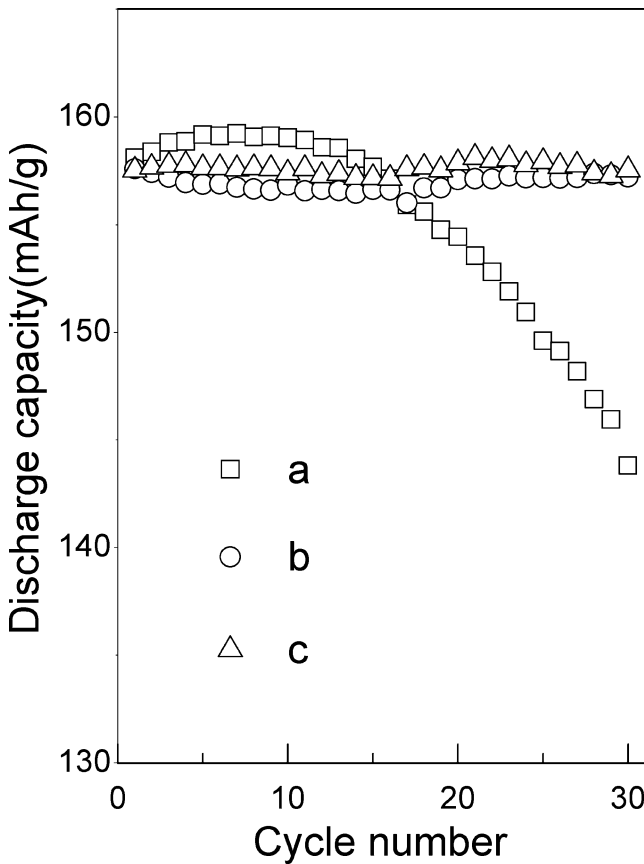


Fig. 3 The continuous charge and discharge curves at 1C during 30 cycles between 3.0 and 4.4 V. (a) Li[Ni_{1/3}Co_{1/3}Mn_{1/3}]O₂; (b) Li[(Ni_{1/3}Co_{1/3}Mn_{1/3})_{0.98}Al_{0.02}]O₂; (c) Li[(Ni_{1/3}Co_{1/3}Mn_{1/3})_{0.96}Al_{0.02}B_{0.02}]O_{1.98}F_{0.02}

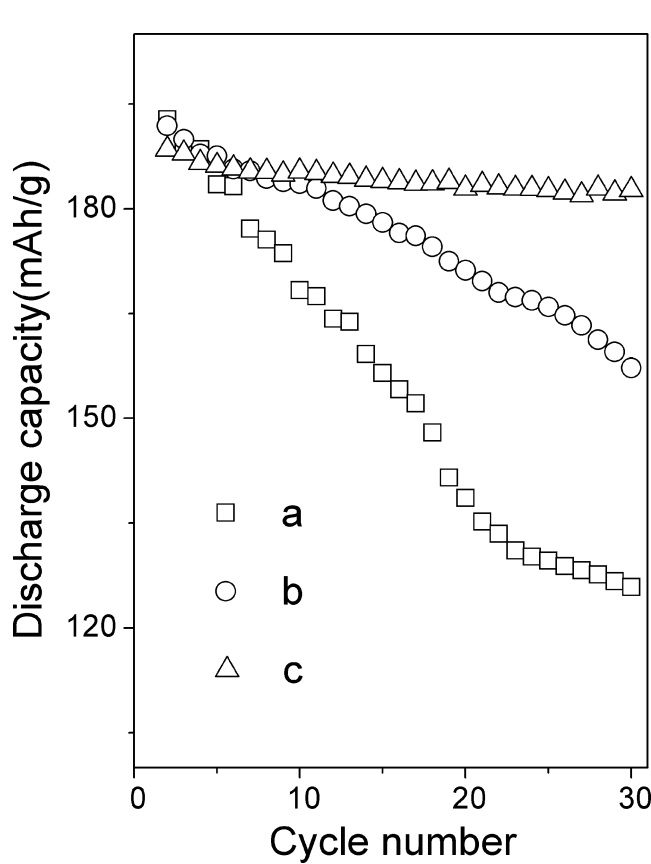


Fig. 4 The continuous charge and discharge curves at 1C during 30 cycles between 3.0 and 4.7 V. (a) Li[Ni_{1/3}Co_{1/3}Mn_{1/3}]O₂; (b) Li[(Ni_{1/3}Co_{1/3}Mn_{1/3})_{0.98}Al_{0.02}]O₂; (c) Li[(Ni_{1/3}Co_{1/3}Mn_{1/3})_{0.96}Al_{0.02}B_{0.02}]O_{1.98}F_{0.02}

$\text{Co}_{1/3}\text{Mn}_{1/3}\text{O}_2$ sample, while Al-doping or Al–B–F-doping can effectively prevent lithium in the transition metal ions layer and restrain nickel in the lithium plane.

Electrochemical tests

Figures 3 and 4 compare the cycling stability of doped and un-doped compounds cycled within preset voltage region at a current rate of 1C. There is no significant difference in the capacity. $\text{Li}[(\text{Ni}_{1/3}\text{Co}_{1/3}\text{Mn}_{1/3})_{0.96}\text{Al}_{0.02}\text{B}_{0.02}]\text{O}_{1.98}\text{F}_{0.02}$ delivered a discharge capacity of 158 mAh/g in the voltage range of 3.0 V and 4.4 V, and 190 mAh/g between 3.0 V and 4.7 V. The most difference was found in the cycling stability: all ion-doped compounds show improved cycling performance compared with that of un-doped compounds. There is no significant difference between Al doped and Al–B–F doped compounds when cycled between 3.0 and 4.4 V (Fig. 3), while it shows much difference when between 3.0 and 4.7 V, as shown in Fig. 4. Un-doped material demonstrated a severe capacity fade in Figs. 3 and 4 and this deterioration is known mainly from cation mixing within the structure [6]. The improvement in the cycling stability of the Al doped or Al–F–B doped sample can be ascribed to no cation mixing, as demonstrated above.

As it is well-known, the capacity at a higher voltage is mainly dependent on the $\text{Co}^{3+/4+}$ redox couple. However, Co^{4+} is significantly unstable in a highly oxidized state, which causes the gradual Co dissolution into the electrolyte. The data in Figs. 3 and 4 show that both Al-doping and Al–F–B-doping can restrain Co dissolution. In the Al doped sample, the capacity retention was much better than that of the un-doped sample $\text{Li}[\text{Ni}_{1/3}\text{Co}_{1/3}\text{Mn}_{1/3}\text{O}_2$ when the cutoff voltage is 4.4 V (Fig. 3). However, as the cutoff voltage operated at 4.7 V, an evident capacity fade was observed (Fig. 4). It is surprising to note that the Al–B–F doped sample showed no significant capacity fade and the higher capacity of 190 mAh/g was maintained during cycling, even though the cell battery cycled to 4.7 V. Kim et al. explained that F-doping can protect the active material from HF attack into the electrolyte at higher voltage operation [12]. We suggest that the better electrochemical performance of the Al-doping or Al–F–B-doping $\text{Li}[\text{Ni}_{1/3}\text{Co}_{1/3}\text{Mn}_{1/3}\text{O}_2$ is attributed primarily to the diminishing cation mixing and consequent stability of the structure. The good reversibility at higher voltage operation (>4.6 V vs Li) may be mainly due to the effect of F-doping in the $\text{Li}[\text{Ni}_{1/3}\text{Co}_{1/3}\text{Mn}_{1/3}\text{O}_2$ cathode.

The volumetric capacity is important for battery applications where the amount of inner space is limited. The volumetric capacities for the doped samples were much higher than that of the un-doped samples even though the gravimetric capacities were similar for the investigated samples (Figs. 3 and 4). The doped powders had higher

tap-densities, especially Al–B–F doped powders and therefore, the corresponding volumetric discharge capacity of the battery was higher.

Conclusions

We have prepared the spherical single phase ion-doped and un-doped $\text{Li}[\text{Ni}_{1/3}\text{Co}_{1/3}\text{Mn}_{1/3}\text{O}_2$ by coprecipitation followed by a high-temperature heat-treatment. Both the tap-density and cycling stability of $\text{Li}[\text{Ni}_{1/3}\text{Co}_{1/3}\text{Mn}_{1/3}\text{O}_2$ are greatly improved by Al–F–B-doping, in particular in the high voltage cycled region. XRD and Rietveld refinement studies indicate that there is no impurity phase formed in the $\text{Li}[(\text{Ni}_{1/3}\text{Co}_{1/3}\text{Mn}_{1/3})_{0.96}\text{Al}_{0.02}\text{B}_{0.02}]\text{O}_{1.98}\text{F}_{0.02}$ sample and the doped samples have well-ordered layered structures with $R\bar{3}m$ space group. Al-doping and F-doping can effectively prevent “cation mixing”.

References

- Ohzuku T, Makimura Y (2001) Layered lithium insertion material of $\text{LiCo}_{1/3}\text{Ni}_{1/3}\text{Mn}_{1/3}\text{O}_2$ for lithium-ion batteries. *Chem Lett* 30:642
- Lu Z, MacNeil DD, Dahn JR (2001) Layered $\text{Li}[\text{Ni}_x\text{Co}_{1-2x}\text{Mn}_x]\text{O}_2$ cathode materials for lithium-ion batteries. *Electrochem Solid-State Lett* 4:A200
- Jouanneau S, MacNeil DD, Lu Z et al (2003) Morphology and safety of $\text{Li}[\text{Ni}_x\text{Co}_{1-x}\text{Mn}_x]\text{O}_2$ ($0 < x < 1$). *J Electrochem Soc* 150: A1299
- Belharouak I, Sun YK, Liu J et al (2003) $\text{Li}(\text{Ni}_{1/3}\text{Co}_{1/3}\text{Mn}_{1/3})\text{O}_2$ as a suitable cathode for high power applications. *J Power Sources* 123:247
- Yabuuchi N, Ohzuku T (2003) Novel lithium insertion material of $\text{LiCo}_{1/3}\text{Ni}_{1/3}\text{Mn}_{1/3}\text{O}_2$ for advanced lithium-ion batteries. *J Power Sources* 119–121:171
- Shaju KM, Subba Rao GV, Chowdari BVR (2002) Performance of layered $\text{Li}(\text{Ni}_{1/3}\text{Co}_{1/3}\text{Mn}_{1/3})\text{O}_2$ as cathode for Li-ion batteries. *Electrochim Acta* 48:145
- Koyama Y, Yabuuchi N, Tanaka I et al (2004) Solid-state chemistry and electrochemistry of $\text{LiCo}_{1/3}\text{Ni}_{1/3}\text{Mn}_{1/3}\text{O}_2$ for advanced lithium-ion batteries. *J Electrochem Soc* 151(10):A1545
- Hwang BJ, Tsai YW, Carlier D et al (2003) A combined computational/experimental study on $\text{LiNi}_{1/3}\text{Co}_{1/3}\text{Mn}_{1/3}\text{O}_2$. *Chem Mater* 15:3676
- Choi J, Manthiram A (2004) Comparison of the electrochemical behaviors of stoichiometric $\text{LiNi}_{1/3}\text{Co}_{1/3}\text{Mn}_{1/3}\text{O}_2$ and lithium excess $\text{Li}_{1.03}(\text{Ni}_{1/3}\text{Co}_{1/3}\text{Mn}_{1/3})_{0.97}\text{O}_2$. *Electrochim Solid-State Lett* 7(10):A365
- Ye SY, Zhang PW, Qiao ZY (2005) Effect of aluminum doping on electrochemical behaviors of layered $\text{Li}[\text{Ni}_{1/3}\text{Co}_{1/3}\text{Mn}_{1/3}\text{O}_2]$ cathode materials. *Trans Nonferrous Met Soc China* 15(S1):30
- Amatucci GG, Pereira N, Zheng T et al (2001) Failure mechanism and improvement of the elevated temperature cycling of LiMn_2O_4 compounds through the use of the $\text{LiAl}_x\text{Mn}_{2-x}\text{O}_{4-y}\text{F}_z$ solid solution. *J Electrochem Soc* 148:A171
- Kim GH, Myung ST, Bang HJ et al (2004) Synthesis and electrochemical properties of $\text{Li}[\text{Ni}_{1/3}\text{Co}_{1/3}\text{Mn}_{(1/3-y)}\text{Mg}_y]\text{O}_{2-y}\text{F}_y$ via coprecipitation. *Electrochim Solid-State Lett* 7(12):A477

13. Jouanneau S, Dahn JR (2003) Preparation, structure, and thermal stability of new $\text{Ni}_x\text{Co}_{1-2x}\text{Mn}_x(\text{OH})_2$ ($0 < x < 1/2$) phases. *Chem Mater* 15:495
14. Jouanneau S, Eberman KW, Krause LJ et al (2003) Synthesis, characterization, and electrochemical behavior of improved $\text{LiNi}_x\text{Co}_{1-x}\text{Mn}_x\text{O}_2$ ($0.1 < x < 0.5$). *J Electrochem Soc* 150: A1637
15. Jouanneau S, Bahmet W, Eberman KW et al (2004) Effect of the sintering agent B_2O_3 , on $\text{Li}[\text{Ni}_x\text{Co}_{1-2x}\text{Mn}_x]\text{O}_2$ materials. *J Electrochem Soc* 151(11):A1789
16. <http://www-lrb.cea.fr/fullweb/fp2k/fp2k.htm>
17. Lu Z, Beaulieu LY, Donaberger RA, Thomas CL, Dahn JR (2002) Synthesis, structure and electrochemical behavior of $\text{Li}[\text{Ni}_x\text{Li}_{1/3-2x/3}\text{Mn}_{2/3-x/3}]\text{O}_2$. *J Electrochem Soc* 149:A778